

Conductance and coherence lengths in disordered carbon nanotubes: Role of lattice defects and phonon vibrations

Stephan Roche,^{1,2} Jie Jiang,² François Triozon,^{1,3} and Riichiro Saito²¹CEA/DSM/DRFMC/SPSMS, 17 avenue des Martyrs, 38054 Grenoble, France²Department of Physics, Tohoku University and CREST-JST, Sendai 980-8578, Japan³CEA/DRT/LETI/D2NT/LSCDP, 17 avenue des Martyrs, 38054 Grenoble, France

(Received 21 July 2005; published 19 September 2005)

We report on a theoretical study of quantum transport in carbon nanotubes in the presence of two different sources of scattering: a static short-range random potential that simulates lattice defects, superimposed onto a long-range time-dependent perturbation that mimics the phonon-induced real-space atomic displacements. In the weak-localization regime, fluctuations of the coherent length scales are shown to be driven by band-structure features, whereas the phonon-induced delocalization effect occurs in the stronger-localization regime.

DOI: 10.1103/PhysRevB.72.113410

PACS number(s): 73.63.Fg, 72.10.Di, 73.23.-b

The theory of localization in disordered mesoscopic systems is a long-standing issue, based on the quantum interference effects (QIE's) on charge transport.^{1,2} These QIE's between clockwise and counterclockwise backscattering paths develop in the so-called coherent regime and yield an increase of the probability of return to the origin for propagating wave packets. The contribution of QIE's is usually reduced by several inelastic scattering sources that produce decoherence of the wave-packet phase. At low temperature the main decoherence mechanisms are electron-phonon and electron-electron couplings. Within the framework of weak-localization theory, it has been possible to derive perturbatively the relation between the measured conductance $G(E)$, its quantum correction $\delta G(E)$, and the coherence length L_ϕ that fixes the scale beyond which QIE's are destroyed. Estimation of the coherence lengths is a central issue in mesoscopic physics, and weak localization provides an elegant framework to extract the behavior of L_ϕ , which mainly depends on the dimensionality of charge transport.^{3,4} Nowadays, an important issue concerns the decoherence phenomenon at very low temperature in disordered metallic systems.¹ The observation of the saturation of the coherence time τ_ϕ ,⁵ despite a vanishing contribution of inelastic backscattering, is challenging the intimate nature of localization in low dimensionality.¹

Within this context, a theoretical characterization of coherence length scales in realistic systems, based on a microscopical modeling of both elastic scatters and a physically sounding long-range time-dependent dephasing perturbation, is missing.

Carbon nanotubes⁶ offer, on the other hand, remarkable opportunities to investigate quantum transport in low-dimensional materials. Weak localization in carbon nanotubes has been the subject of intense research during recent years. At first, large-diameter nanotubes were shown to manifest a negative magnetoresistance effect (decreasing of the resistance upon switching on an external magnetic field) as well as Aharonov-Bohm oscillations with a half-quantum-flux period.⁷ Recently weak localization was also observed in small-diameter double-walled nanotubes with external diameter of only ~ 3 nm.⁸ The nature of intrinsic lattice defects is,

however, difficult to analyze experimentally, but the use of the so-called Anderson-type random potential has allowed a reasonable interpretation of experiments.⁸ Finally, Stojetz and co-workers⁹ have recently succeeded in measuring some energy dependence of the coherence length scale by using an efficient back-gate electrode able to move the Fermi-level position and explore the physics of different subbands. Their measurements show a systematic decrease of L_ϕ near the onsets of new subbands (van Hove singularity positions).

In this paper, we study quantum transport in *weakly disordered carbon nanotubes in the presence of electron-phonon coupling*. Our numerical approach consists in computing the time-dependent quantum dynamics of electronic wave packets (for π electrons), under the action of a time-dependent Hamiltonian that mimics the vibrational modes in real space as well as the strength of the electron-phonon coupling. For selected phonon modes (acoustic and optical), the time-dependent Schrödinger equation is solved in real space¹⁰ and the Kubo conductance³ as well as coherence length scales are investigated in the weak-localization regime.⁴ Remarkably, for strong static disorder, long-range vibrations are shown to limit localization effects.

The starting Hamiltonian is the π effective model

$$\hat{\mathcal{H}} = \sum_i \varepsilon_i |\pi_i\rangle \langle \pi_i| + \sum_{i,\delta=1,3} \gamma(r_{i,i+\delta}) [|\pi_i\rangle \langle \pi_{i+\delta}| + \text{H.c.}],$$

where the on-site energies ε_i are taken at random within the interval $[-W/2, W/2]$ (with uniform probability, while W is in $\gamma_0=2.7$ eV units) to simulate lattice defects (Anderson-type disorder potential),¹¹ whereas the integral overlaps between nearest-neighbor orbitals $|\pi_i\rangle$ and $|\pi_{i+\delta}\rangle$ are constant ($\gamma_{i,i+\delta}=\gamma_0$) in the absence of phonon vibrations. The effect of the electron-phonon interaction is introduced by modulating the integral overlap intensity $\gamma(r_{i,i+\delta})$ according to the time-dependent displacements of the bond lengths $r_{i,i+\delta}$ between one $|\pi_i\rangle$ orbital located at atomic position $|i\rangle$ and its nearest neighbors located at $|i+\delta\rangle$ ($\delta \in [1,3]$). The bond-length-dependent Hamiltonian matrix element γ is computed by using the analytical expression given by Porezag *et al.*¹² The C-C bond length is therefore $r_{i,i+\delta} = \hat{\delta} \cdot (\mathbf{R}_{i+\delta} - \mathbf{R}_i)$, with $\hat{\delta}$ the

bond direction. The atomic position for the phonon mode with wave vector \mathbf{q} and frequency $\omega_{\mathbf{q}}$ is given by $\mathbf{R}_i = \mathbf{R}_i^0 + A_{\mathbf{q}} \mathbf{e}_{\mathbf{q}}(\mathbf{q}) \cos(\mathbf{q} \cdot \mathbf{R}_i + \omega_{\mathbf{q}} t)$, where \mathbf{R}_i^0 give the equilibrium atomic positions, whereas A and \mathbf{e} are the phonon amplitude and eigenvector. The phonon amplitude is given by $A_{\mathbf{q}} = \sqrt{\hbar n_{\mathbf{q}} / 2M\omega_{\mathbf{q}}}$, where M is the carbon mass, while $n_{\mathbf{q}}$ is the phonon occupation number. For thermal equilibrium, $n_{\mathbf{q}}$ is the Bose-Einstein occupation factor, $n_{\mathbf{q}} = 1 / (e^{\beta\epsilon} - 1)$ for phonon absorption and $n_{\mathbf{q}} = 1 / (e^{\beta\epsilon} - 1) + 1$ for phonon emission with $\beta = k_B T$ and ϵ phonon energy.¹³ Hereafter we will concentrate on the longitudinal acoustic (LA) phonon mode and longitudinal optical (LO) mode, with the oscillation amplitude defined by A_0 .

The resolution of the time-dependent Schrödinger equation is made by expanding the evolution operator $e^{-i\hat{H}t}$ as a product of short-time evolution steps $e^{-i\hat{H}\Delta T}$, for a total evolution time $t = n\Delta T$. Typically ΔT is one-tenth of the oscillation period of the considered phonon mode. During each elapsed time ΔT , the Hamiltonian energetics is fixed by the static part of the Anderson potential, whereas the time-dependent part, due to long-range vibrational modes, varies following the real space modulations of the overlap integrals. A similar treatment of dephasing has been implemented either by defining an artificial oscillating behavior of off-diagonal electronic couplings¹⁴ or through an on-site time-dependent perturbation.¹⁵ In Ref. 14, scaling properties of the quantum conductance were analyzed in the weak-localization regime, whereas the metal-insulator transition was investigated in Ref. 15.

The Kubo conductance is related to the diffusion coefficient $\text{Tr}\{\delta(E - \hat{H})[\hat{\chi}(t) - \hat{\chi}(0)]^2\} / \text{Tr}[\delta(E - \hat{H})]$, where $\delta(E - \hat{H})$ is the spectral measure operator, whose trace gives the total density of states, while $\hat{\chi}(t)$ is the position operator in the Heisenberg representation. From the time dependence of $L^2(E, t) = \langle \Psi(0) | [\hat{\chi}(t) - \hat{\chi}(0)]^2 | \Psi(0) \rangle$, one derives the scaling properties of the conductance,¹⁰ together with the conduction regime. The presence of lattice defects produces elastic scattering of the π electrons and leads to a transition of the quantum spreading from a ballistic like to a diffusive regime, at which the diffusion coefficient will first saturate. This allows us to estimate the intrinsic elastic mean free path from $L^2(E, t) / t \rightarrow \ell_e v(E)$ for a given disorder strength.

In the top panel of Fig. 1, the elastic mean free path is shown for three amplitudes of the disorder potential $W = \{0.07, 0.1, 0.5\}\gamma_0$. Close to the charge neutrality point, $\ell_e(E=0)$ can be derived analytically within the Fermi golden rule (FGR). The use of the Fermi golden rule gives $\ell_e = v_F \tau_e$, with $v_F = 3a_{cc}\gamma_0 / 2\hbar$ the Fermi velocity ($a_{cc} = 1.44 \text{ \AA}$), whereas τ_e is the elastic scattering time. For the Anderson disorder potential, an analytical derivation gives¹¹

$$\ell_e = \frac{18a_{cc}\gamma_0^2}{W^2} \sqrt{n^2 + m^2 + nm}. \quad (1)$$

The obtained values for ℓ_e at the charge neutrality point are given by $\ell_e(E=0, W=0.05\gamma_0) = 2800 \text{ nm}$, $\ell_e(E=0, W=0.1\gamma_0) = 800 \text{ nm}$, and $\ell_e(E=0, W=0.5\gamma_0) = 37 \text{ nm}$. Note that

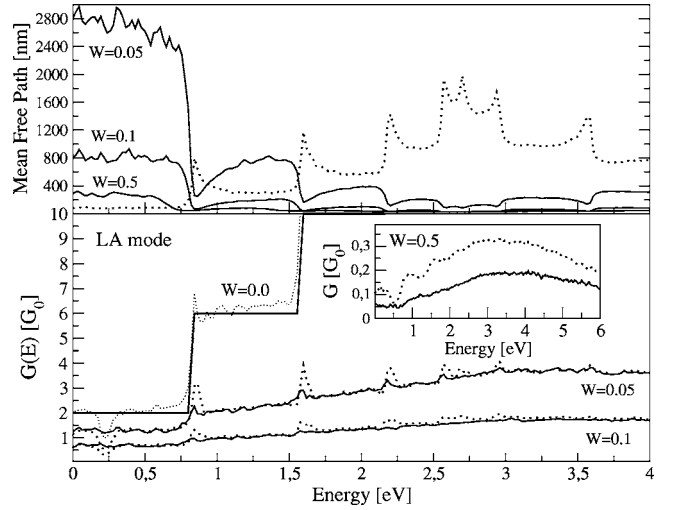


FIG. 1. Top panel: elastic mean free path for a metallic (10,10) disordered nanotube as a function of energy of charge carriers and for several values of the Anderson random potential W given in γ_0 units. Note that $\ell_e(W=0.5)$ has been rescaled by a factor of 8. The rescaled density of states (dotted line) is also shown. Bottom panel: corresponding conductance (main frame) with elastic disorder and electron-phonon time-dependent dephasing. The staircase gives the exact number of quantum channels, N_{\perp} . Inset: conductance for a larger value of the disorder potential $W=0.5\gamma_0$ with (dotted line) or without (bold line) LA-mode displacements.

in Fig. 1, $\ell_e(W=0.5\gamma_0) \rightarrow 8\ell_e(E=0, W=0.5\gamma_0)$, for the sake of clarity. One thus finds that $\ell_e(W=0.05) / \ell_e(W=0.1) \approx 3.5$, whereas $\ell_e(W=0.05) / \ell_e(W=0.5) \approx 80$, in good agreement with the $1/W^2$ scaling given by Eq. (1). At higher energies, ℓ_e decreases significantly with some modulations at the onsets of new subbands.

By defining $\tau(L)$ the time at which $L^2(t) = L^2$, the conductance at such a scale is defined by $G \approx e^2 n(E) L(\tau(L)) / \tau(L)$.¹⁰ In Fig. 1 (bottom panel), the quantum conductance is shown for the same parameters for the random potential but with superimposition of the additional time-dependent part encoding the LA mode. At $W=0.0$ the effect of phonon vibrations is negligible in most of the spectrum except at some particular energies $\pm 0.2 \text{ eV}$, which correspond to a particular phonon-induced symmetry breaking effect.^{16,17} For disorder $W = \{0.07, 0.1\}\gamma_0$, the conductance takes values much smaller than in the ballistic case [$W=0$ and $G(E) = N_{\perp} G_0$, with N_{\perp} the number of available channels, $G_0 = 2e^2/h$], and the superimposed effect of phonons remains weak. In contrast, for a sufficiently large potential strength ($W=0.5\gamma_0$), a remarkable increase of the conductance due to phonon-induced atomic displacements is seen for all the spectrum (Fig. 1, bottom panel, inset). Such a *dephasing-assisted limitation of localization effects* has already been discussed in other models,¹⁸ but it is here disclosed for realistic quasi-one-dimensional (quasi-1D) systems and physical modeling of the time-dependent perturbation that mimics a real phenomenon (lattice vibrations).

To extract the information about the energy dependence of the coherence length scales, we proceed as follows. In the weak-localization regime, the quantum correction of the

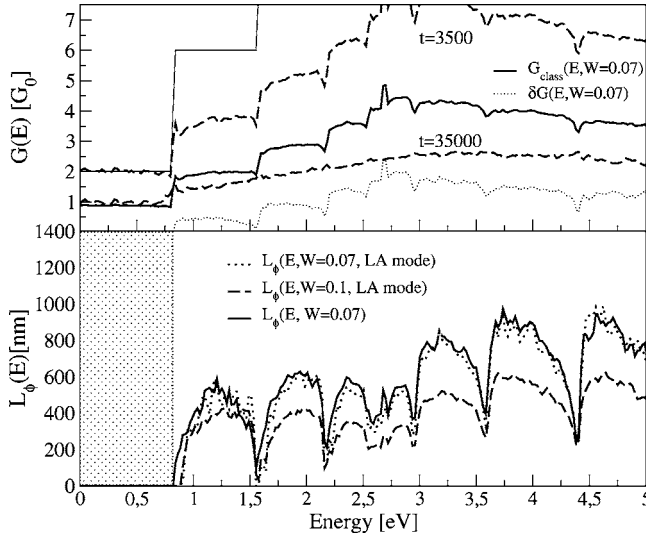


FIG. 2. Top panel: conductance for the disordered (10,10) tube with $W=0.07\gamma_0$, taken at evolution times $t=3500\hbar/\gamma_0$ and $t=35000\hbar/\gamma_0$ (dashed curves). The bold curve gives the classical part $G_{\text{class}}(E)=G_0 N_{\perp} \ell_e(E)/L(E,t)$, whereas the dotted curve gives the quantum correction $\delta G(E)$ ($t=35000\hbar/\gamma_0$). Bottom panel: coherence lengths deduced from $\delta G(E)=L_{\phi}(E)/L(E)$ computed at $t=35000\hbar/\gamma_0$ and for several values of the disorder potential. The dotted region is not addressed since $\delta G(E)\approx 0$ at $t=35000\hbar/\gamma_0$.

Drude conductance is computed by solving the so-called Cooperon equation.⁴ Assuming a quasi-1D geometry of the system, it has been shown that decoherence due either to electron-phonon or electron-electron scattering is described by the same approach^{19,20} and that the conductance reads

$$G(E) = \frac{2e^2}{h} \left(N_{\perp}(E) \frac{\ell_e(E)}{L(E,t)} - \delta G(E) \right), \quad (2)$$

where $L(E,t)$ is the length scale that is energy dependent due to velocity $v(E)$ and scales as $L(E,t)=\sqrt{v(E)\ell_e t}$, in the diffusive regime, whereas the term $\delta G(E)$ gives the contribution of QIE's beyond the scale of ℓ_e . Within the weak-localization theory and for quasi-1D systems, this contribution is shown to be related to the coherence length $L_{\phi}(E)$ as $\delta G(E)=L_{\phi}(E)/L(E,t)$, whereas $\tau_{\phi}(E)=L_{\phi}^2(E)/v(E)\ell_e$. Therefore, by studying the scaling behavior of $\delta G(E)$, one can access relevant physical information about the fluctuations of the coherence length scales in the weak-localization regime.

Figure 2 (top panel) shows the conductance computed at two different evolution times $t=3500\hbar/\gamma_0$ and $t=35000\hbar/\gamma_0 \approx 8$ ps (dashed curves). One clearly sees a downscaling of the conductance with time, which comes from the classical linear downsizing in the diffusive regime $\ell_e(E)/L(E,t)$, together with the QIE contribution of $\delta G(E,t)$, which increases with time, since interferences are allowed to develop on a larger scale. In the same figure, one also reports the classical term $G_{\text{class}}(E)=N_{\perp}(E)G_0\ell_e(E)/L(E,t)$ (bold curve), along with the quantum interference term $\delta G(E,t)=G(E,t)-G_{\text{class}}(E)$ (dotted curve), at $t=35000\hbar/\gamma_0$. These results are obtained for $W=0.07\gamma_0$ and no phonon dephasing.

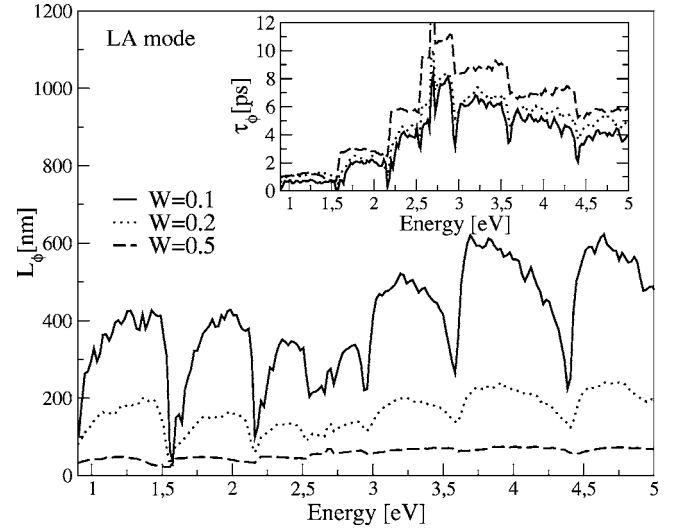


FIG. 3. Main frame: coherence length as a function of energy for random potential of $W=0.1\gamma_0$ (bold curve), $W=0.2\gamma_0$ (dotted curve), and $W=0.5\gamma_0$ (dashed curve). Inset: corresponding $\tau_{\phi}(E)$ for the same parameters. In addition to the random short-range disorder, a LA-mode modulation is introduced.

Figure 2 (bottom panel) gives $L_{\phi}(E)$ deduced from Eq. (2) for $W=\{0.07,0.1\}\gamma_0$, with (dashed and dotted curves) and without (bold curve) phonon dephasing. The values range within [10 nm, 1000 nm] in the considered energy window. One notes that for energies ≤ 0.9 eV and within the considered evolution time, the quantum correction $\delta G(E)\approx 0$, so that no meaningful information about the coherence length can be deduced in the weak-localization regime. In Fig. 3, stronger static disorder potentials are considered. The results show the important decrease of the coherence length with elastic disorder. In contrast, the coherence time $\tau_{\phi}(E)$ (inset) shows reversed behavior, owing to the strong decrease of ℓ_e .

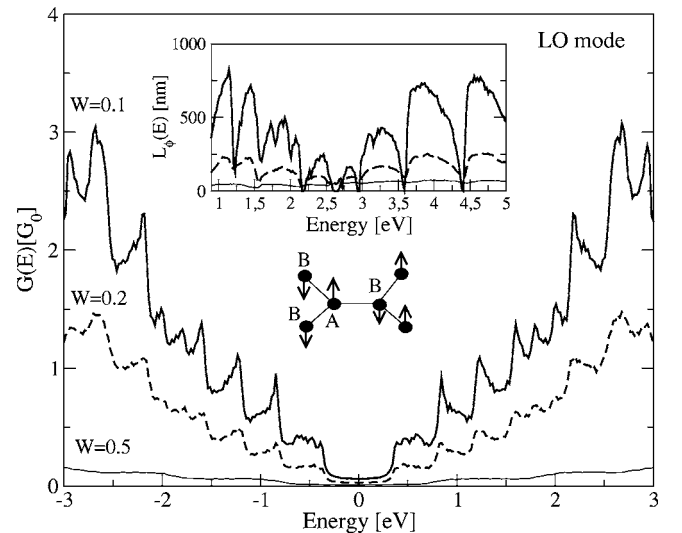


FIG. 4. Main frame: conductance of disordered (10,10) nanotubes in the presence of the superimposed phonon-dephasing term due to the LO phonon mode. A drawing gives the relative atomic displacements between first neighbors. Inset: $L_{\phi}(E)$ for the same parameters at $t=35000\hbar/\gamma_0$.

In the experimental situation,⁹ the fluctuations of $L_\phi(E)$ due to electron-electron scattering were found to scan the range [10 nm, 60 nm], with a systematic decrease near the onsets of new subbands. The values given here (for the chosen evolution time) are thus physically reasonable, since electron-phonon scattering is expected to lead to a weaker decoherence effect.^{20,21}

In Fig. 4, the conductance for several random potentials and a superimposed longitudinal optic (LO) phonon dephasing are reported. Differently from the LA mode, the LO-mode-driven dephasing impacts more significantly at lower energies, close to the charge neutrality point, and its introduction yields strong modulation of the conductance close to the onsets of new subbands. The strong reduction of $G(E)$ within $[-0.5 \text{ eV}, 0.5 \text{ eV}]$, has been shown in Refs. 16 and 17 to come from time-dependent band-structure changes driven by the LO vibrational modes. Similarly to the prior case, $L_\phi(E)$ is seen to decrease at each onset of a new subband and is strongly affected by increasing the static disorder potential.

In conclusion, the combined effect of static short-range and dynamic long-range disorder has been studied, simulating the case of disordered carbon nanotubes in the presence of vibrational degrees of freedom. In the weak-localization regime, coherence length scales were shown to fluctuate in accordance with the spectral features, while in the case of a strong static potential, the time-dependent long-range perturbation was shown to induce delocalization effects. *Ab initio* molecular dynamics was recently used to study the role of phonon dephasing on elastic scattering and conductance in short nanotube-based junctions.²² Our present approach and results provide a complementary framework to understand localization phenomena in carbon nanotubes in the presence of vibrational modes.

S.R. acknowledges support from ACI grants Transnanofils and NOCIEL, and the CREST/JST for supporting his work in Japan. R.S. acknowledges a Grant-in-Aid (No. 16076201) from the Ministry of Education, Japan. S.R. is indebted to X. Blase and Ch. Strunk for stimulating discussions.

-
- ¹D. J. Thouless, Phys. Rev. Lett. **39** 1167 (1977); E. Abrahams *et al.*, *ibid.* **42**, 673 (1979).
²B. L. Altshuler and A. G. Aronov, in *Electron-Electron Interactions in Disordered Systems*, edited by A. L. Efros and M. Pollak (North-Holland, Amsterdam, 1985), p. 1.
³M. J. Kearney and P. N. Butcher, J. Phys. C **21**, 2539 (1988).
⁴E. Akkermans and G. Montambaux, *Physique Mésoscopique des Électrons et des Photons* (EDP Sciences, Paris, 2004).
⁵P. Mohanty, E. M. Q. Jariwala, and R. A. Webb, Phys. Rev. Lett. **78**, 3366 (1997).
⁶R. Saito, G. Dresselhaus, and M. Dresselhaus, *Physical Properties of Carbon Nanotubes* (Imperial College Press, London, 1998).
⁷C. Schönberger *et al.*, Appl. Phys. A: Mater. Sci. Process. **69** 283 (1999).
⁸G. Fedorov *et al.*, Phys. Rev. Lett. **94**, 066801 (2005).
⁹B. Stojetz *et al.*, Phys. Rev. Lett. **94**, 186802 (2005).
¹⁰S. Roche and R. Saito, Phys. Rev. Lett. **87**, 246803 (2001); F. Triozon *et al.*, Phys. Rev. B **69**, 121410 (2004); S. Latil *et al.*, Phys. Rev. Lett. **92**, 256805 (2004).
¹¹C. T. White and T. N. Todorov, Nature (London) **393**, 240 (1998); P. L. McEuen *et al.*, Phys. Rev. Lett. **83**, 5098 (1999); S. Roche, G. Dresselhaus, M. S. Dresselhaus, and R. Saito, Phys. Rev. B **62**, 16092 (2000).
¹²D. Porezag, Th. Frauenheim, Th. Köhler, G. Seifert, and R. Kaschner, Phys. Rev. B **51**, 12947 (1995).
¹³P. K. Lam, M. M. Dacorogna, and M. L. Cohen, Phys. Rev. B **34**, 5065 (1986).
¹⁴H. Watanabe *et al.*, J. Phys. Soc. Jpn. **72**, 645 (2003).
¹⁵D. A. Evensky, R. T. Scalettar, and P. G. Wolynes, J. Phys. Chem. **94**, 1149 (1990); T. Nakanishi, T. Ohtsuki, and T. Kawarabayashi, J. Phys. Soc. Jpn. **66**, 949 (1997).
¹⁶M. Máchon *et al.*, Phys. Rev. B **71**, 035416 (2005); J. Jiang *et al.*, *ibid.* **71**, 045417 (2005); S. Reich *et al.*, *ibid.* **71**, 033402 (2005).
¹⁷S. Roche, J. Jiang, F. Triozon, and R. Saito, Phys. Rev. Lett. **95**, 076803 (2005).
¹⁸H. Yamada and K. S. Ikeda, Phys. Rev. E **65**, 046211 (2002).
¹⁹A. Stern, Y. Aharonov, and Y. Imry, Phys. Rev. A **41**, 3436 (1990).
²⁰S. Chakraverty and A. Schmid, Phys. Rep. **140**, 193 (1986).
²¹H. Suzuura and T. Ando, Phys. Rev. B **65**, 235412 (2002); V. Perebeinos, J. Tersoff, and Ph. Avouris, Phys. Rev. Lett. **94**, 086802 (2005); Ji-Yong Park *et al.*, Nano Lett. **4**, 517 (2004); X. Blase *et al.*, Phys. Rev. Lett. **93**, 237004 (2004).
²²M. Gheorge *et al.*, Europhys. Lett. **71**, 438 (2005).